

Growth and characterization of a novel In_2Se_3 structure

C. H. de Groot^{a)} and J. S. Moodera

Francis Bitter Magnet Laboratory, Massachusetts Institute of Technology, 170 Albany Street, Cambridge, Massachusetts 02139

(Received 6 September 2000; accepted for publication 23 January 2001)

Thin films of In_2Se_3 deposited by thermal co-evaporation crystallize upon vacuum annealing almost single phase into an, up to now, unknown structure. Only when the films are capped with a thin oxide layer before annealing, the reportedly stable $\gamma\text{-In}_2\text{Se}_3$ structure, single phase and aligned along the c axis forms. Rutherford backscattering confirms an In to Se ratio of 2 to 3 for both structures. Nevertheless, the new structure has distinct x-ray diffraction peaks and Raman spectra. The new structure has a much lower resistivity than the $\gamma\text{-In}_2\text{Se}_3$ structure, consistent with its smaller electrical and optical energy gap. Both structures show large photoconductivity. © 2001 American Institute of Physics. [DOI: 10.1063/1.1355287]

I. INTRODUCTION

Binary chalcogenide alloys of the type $\text{III}_2\text{-VI}_3$, with group VI elements S, Se, and Te have been widely studied during the last decade and the potential application of In_2Se_3 as an absorber material in a photovoltaic cell^{1,2} has revived interest in this compound. Like most of the $\text{III}_2\text{-VI}_3$ compounds, In_2Se_3 has a tetrahedral bonding structure and is a semiconductor material. In addition, in order to satisfy the octet rule for sp^3 hybridization, one third of the cation sites are vacant.³ Although the structural, electronic and optical properties of In_2Se_3 are studied by many groups,⁴⁻¹⁵ the results are rather confusing and contradictory, because most measurements have been done on multiphase films. The problems associated with preparing single-phase films, are the many different crystalline phases that exist for In_2Se_3 , the numerous other In–Se compounds, as well as the high vapor pressure of Se. The large influence that the microstructure and secondary phases (surface layers) may have on the transport properties contributes further to the confusion. In this article, the properties of In_2Se_3 thin films are investigated, carefully taking the above facts into consideration.

II. EXPERIMENT

In_2Se_3 films are deposited by stoichiometric coevaporation from elemental sources in a high vacuum chamber with resistively heated W boats (for Se and dopants) and two electron guns (for In and Al_2O_3 or MgO). The base pressure was $\leq 1 \times 10^{-5}$ Pa. Evaporation rates, typically 0.1 nm/s, are controlled independently by three quartz crystal monitors. Film thickness ranged from 40 to 200 nm. A 3 nm Al_2O_3 or MgO layer was deposited on top of some of the films. The films are subsequently annealed *in situ* for 1 h at 340 °C in a 100 Pa argon atmosphere. To stabilize different crystal structures dopants, such as Ag, Sb, and Te, were substituted by coevaporation from another W boat. Rigaku systems with

$\text{Cu } k\alpha$ radiation were used for x-ray diffraction (also at high temperature), Rutherford backscatter spectroscopy was employed for compositional analysis, and a Cary 5 spectrometer for optical measurements. Resistance and photocurrent were measured on a film with predeposited Pt electrodes and a well defined junction area of 1 mm² with an electrometer (Keithley 6514) and a 0.95 mW HeNe laser (Unisource). Raman spectroscopy has been performed on a Kaiser Hololab 5000 series.

III. RESULTS AND DISCUSSION

A. Structural characterization

In Fig. 1, x-ray diffraction data are shown for two 200 nm In_2Se_3 films that are annealed *in situ* at 340 °C for 1 h in an argon atmosphere. The difference between the films is a 3 nm MgO protection layer that has been deposited on film A before annealing. This film A correspond to the well known $\gamma\text{-In}_2\text{Se}_3$ structure. It is single phase and has a perfect alignment along the c axis. Similar films have been grown consistently by others by multilayer deposition of In and Se.^{14,15}

When the In_2Se_3 films are annealed without a protective layer, a completely different x-ray pattern arises. Except for the small peak due to the $\gamma\text{-006}$ reflection, the peaks, displayed in Table I, do not correspond to any known phase of the In–Se phase diagram, although peaks at some of those positions have been reported, unindexed, in an InSe hydrate¹⁶ and in $\text{In}_2\text{Zn}_{0.4}\text{Se}_3$.¹⁷ The x-ray pattern corresponds to a single inter planar spacing and can be indexed with consecutive 00 l peaks.

The reproducibility of this pattern, including the ratio of the peak heights, strongly indicates that the film is single phase and that the indexing is basically correct. This indexing would correspond to a lattice parameter in the c direction of 1.99 nm, an increase of 3% with respect to $\alpha\text{-In}_2\text{Se}_3$ or $\gamma\text{-In}_2\text{Se}_3$. Peculiar is the high intensity of 00 l peaks with odd l , 003 and 005 being the largest peaks. These spacings are usually systematic extinctions due to symmetry considerations, as they are in all other In_2Se_3 phases. However, a strongly distorted structure might give rise to symmetry breaking. A doubling of the proposed lattice spacing would

^{a)}Present address: Electronics and Computer Science Department, University of Southampton, Southampton, U.K.; electronic mail: chdg@ecs.soton.ac.uk

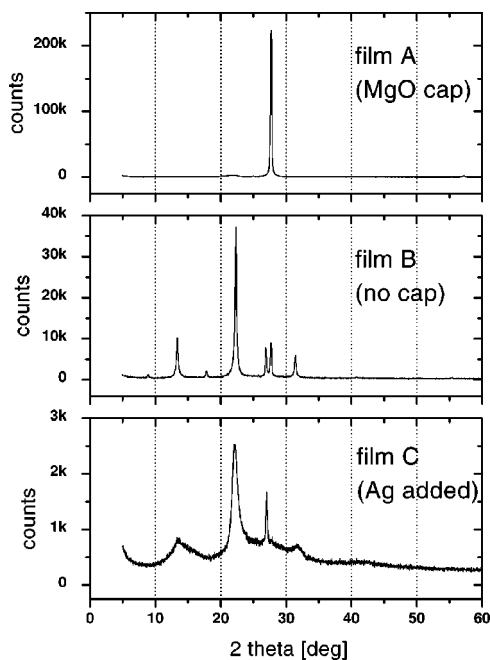


FIG. 1. X-ray diffraction spectra of γ - In_2Se_3 (A) and the novel In_2Se_3 structure (B). Both films are 200 nm thick and annealed *in situ*; the only difference is that the γ - In_2Se_3 film has a 3 nm MgO cap layer deposited on top before annealing. (C) $\text{In}_2\text{Se}_3\text{Ag}_{0.2}$ film with a cap layer showing broadened peaks of the novel structure

off course eliminate peaks with odd l , but this will not facilitate any explanation.

It should be noted that a lot of confusion is due to different assignments for identical In_2Se_3 structures and vice versa. As argued by Ye *et al.*,⁴ there exist only two structures; a layered structure (α - In_2Se_3) best characterized by PCDFS 40-1408 and a defect wurtzite structure (γ - In_2Se_3) described by PCDFS 40-1407. The novel structure discussed here is distinct from both and will be referred to as κ - In_2Se_3 for the time being.

To probe the crystallization of the In_2Se_3 films, x-ray diffraction scans were conducted while stepwise increasing the temperature of an amorphous film on a hot stage under Ar atmosphere. In the capped films, the onset of γ - In_2Se_3 formation occurs at 180 °C as shown in Fig 2. Remarkably, annealing *ex situ* of the amorphous uncapped In_2Se_3 films does not result in the formation of the κ - In_2Se_3 structure; The films crystallize predominantly or completely in the γ - In_2Se_3 structure, even when annealed in air instead of argon. Annealing of (already *in situ* annealed) κ - In_2Se_3 leads

TABLE I. X-ray diffraction peaks of the novel (κ -) In_2Se_3 structure with the proposed indexing, assuming a c -axis lattice spacing of 1.99 nm.

2θ (deg)	d (pm)	I/I_{max}	hkl
8.91	992.0	0.02	002
13.36	662.3	0.26	003
17.82	497.3	0.04	004
22.33	397.9	1.00	005
26.92	331.0	0.19	006
27.68	322.0	var	γ 006
31.44	284.3	0.15	007

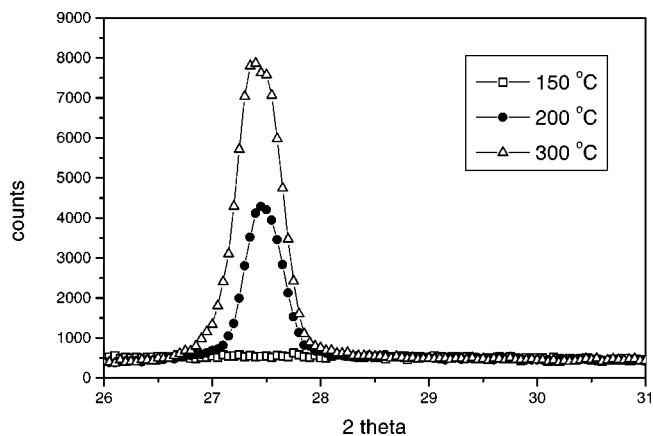


FIG. 2. X-ray diffraction pattern of an (amorphous) In_2Se_3 film at various temperatures during the annealing in argon. The peak corresponds to the 006 peak of γ - In_2Se_3 . The onset of crystallization occurs at 180 °C.

to a disappearance of this structure in favor of γ - In_2Se_3 formation at approximately the same temperature at which γ - In_2Se_3 forms from the amorphous phase. Upon prolonged heating at higher temperatures (400 °C) in air, the uncapped γ - In_2Se_3 transforms completely to (transparent conductor) In_2O_3 with no evidence of Se, and no intermediate compound is formed during that process.

We have tried to influence the growth of the different In_2Se_3 structures in different ways by varying the evaporation ratio (In_2Se_x with $2.8 \leq x \leq 4$), substrate (soda-lime glass, quartz, oxidized Si and Al_2O_3), substrate temperature (ambient and 100 °C), capping layer (MgO and Al_2O_3), and by changing the annealing atmosphere from Ar to vacuum. None of these actions influenced the formation of the different In_2Se_3 structures. Only by adding small amounts of foreign elements could the crystalline structure be changed and made independent whether the film has been capped or not. Sb substituted for In stabilized the α - $\text{In}_{2-x}\text{Sb}_x\text{Se}_3$ structure ($0.05 \leq x \leq 1$) in agreement with Ref. 18 and Te substituted for Se stabilized the γ - $\text{In}_2\text{Se}_{3-x}\text{Te}_x$ structure for $0.1 \leq x \leq 0.5$ (see also Ref. 19).

The noble metals Ag and Cu do not substitute easily in In–Se but are prone to form compounds (e.g., the CuInSe_2 photovoltaic absorbers). It turned out, however, that small amounts of Ag addition stabilize the κ - $\text{In}_2\text{Se}_3\text{Ag}_x$ structure for $x \leq 0.2$ in the sense that the κ - In_2Se_3 structure formed both with and without capped films, although with considerably broadened peaks [see Fig. 1(C)]. The peaks do not belong to any of the chalcopyrite phases. It is possible that Ag atoms substitute for one of the constituents, but it is more likely that it fills structural vacancies.

The most obvious explanation for the difference in structure between the capped and uncapped structure is the evaporation of Se during annealing. However, as is shown in Fig. 3, Rutherford backscatter spectroscopy (RBS) on 40 nm films shows that the Se/In ratio is 1.50 ± 0.01 for both structures, proving the absence of any noticeable Se evaporation. From the similar shape of the RBS spectra, it may also be concluded that no large scale segregation of the elements takes place. In 200 nm films, the Al of the capping layer is

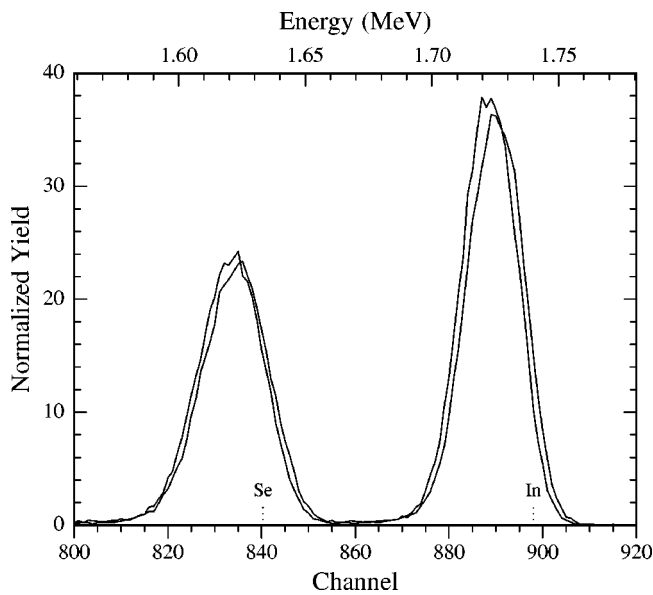


FIG. 3. RBS spectra of 40 nm γ - In_2Se_3 and κ - In_2Se_3 films. Analysis of the peak areas confirms that the Se/In ratio in the films is 1.50 ± 0.01 for both structures. The γ - In_2Se_3 spectrum is shifted to slightly lower energy values due to the stopping power of the Al_2O_3 cap.

visible separately, because the Si substrate peak is pushed to lower energies. This shows that the Al_2O_3 or MgO remains on top and does not diffuse into the film during annealing.

The x-ray diffraction in the hot stage shows that the κ - In_2Se_3 structure transforms to γ - In_2Se_3 upon annealing. However, *in situ* annealing reveals that the κ - In_2Se_3 structure is also stable at elevated temperatures. The formation of γ - In_2Se_3 in uncapped *ex situ* annealed films can hence only be explained by assuming that surface oxidation (which happens inevitably) also acts as a cap layer. Notice that in experiments of other authors, the In_2Se_3 films are either annealed *ex situ* or deposited as a multilayer in which the top layer can act as a cap layer. Our results are hence not in conflict with previous experiments. To understand the role of the cap layer, one has to assume that film crystallization starts at the surface. The precise role of the cap layer is, however, unclear. It might act as a template for γ - In_2Se_3 or its absence might change the surface composition favoring crystallization of κ - In_2Se_3 seeds.

Even though the x-ray diffraction peaks show a distinct structure, the molecular environment of the new structure might be very similar to one of the known In_2Se_3 structures. Raman spectrometry (Fig. 4) shows that the characteristic peak of γ - In_2Se_3 at 150 cm^{-1} is also present in κ - In_2Se_3 , although less pronounced, and we can hence conclude that the molecular structure is rather similar. All In_2Se_3 structures can be considered as defect structures where the structural vacancies behave as one atomic species.³ An explanation for the κ - In_2Se_3 might be that the reordering of these vacancies will slightly change the lattice parameters and destroy the high symmetry of the γ - In_2Se_3 , leading to very distinct x-ray diffraction peaks.

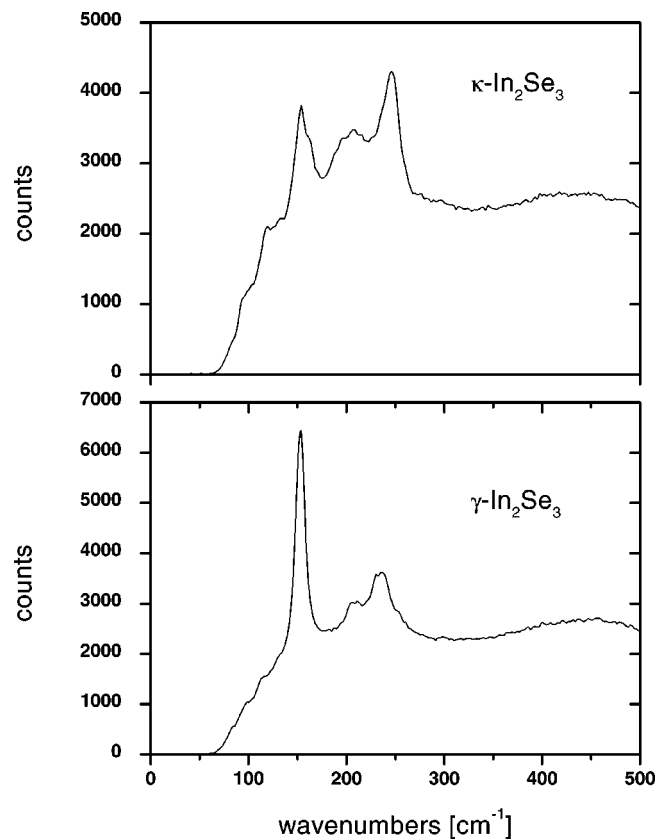


FIG. 4. Raman spectra for 200 nm κ - In_2Se_3 and γ - In_2Se_3 films. The wavelength of the diode laser is 633 nm. The γ - In_2Se_3 structure is readily identified by the large peak at 150 cm^{-1} . The κ - In_2Se_3 structure has a distinct but similar pattern.

B. Electrical and optical characterization

The resistivity and photoconductivity of κ - In_2Se_3 and γ - In_2Se_3 has been measured on glass substrates with Pt electrodes. The ohmic resistivity of $2 \times 10^7 \Omega \text{ cm}$ for γ - In_2Se_3 is comparable to the class of high-resistance films in Ref. 14 and higher than those values reported by others (on mostly multiphase films). The κ - In_2Se_3 films show considerably lower resistivity on the order of $1 \times 10^5 \Omega \text{ cm}$. The temperature dependence of both structures follows an Arrhenius behavior over a wide temperature range as can be seen in Fig. 5. The κ - In_2Se_3 shows an activation energy E_A of 0.43 eV in the temperature range from 150 to 400 K. γ - In_2Se_3 shows linear behavior up to 450 K [the high resistance ($T\Omega$) prevented accurate measurements below room temperature], with E_A 0.68 eV. Both structures show large photoconductivity with slow decay on the scale of minutes. For the κ - In_2Se_3 films, the photocurrent is more than 2 orders of magnitude larger than the dark current corresponding to more than 10 mA/W photocurrent (see Table II). The relatively small temperature dependence shows that the measured photoconductivity cannot be due to heating of the film, as this would translate to a temperature rise of over 100°C , a highly unlikely number considering the low power density of the laser source. The large photoconductivity also shows that the resistivity of the κ - In_2Se_3 is not due to a shunt by a

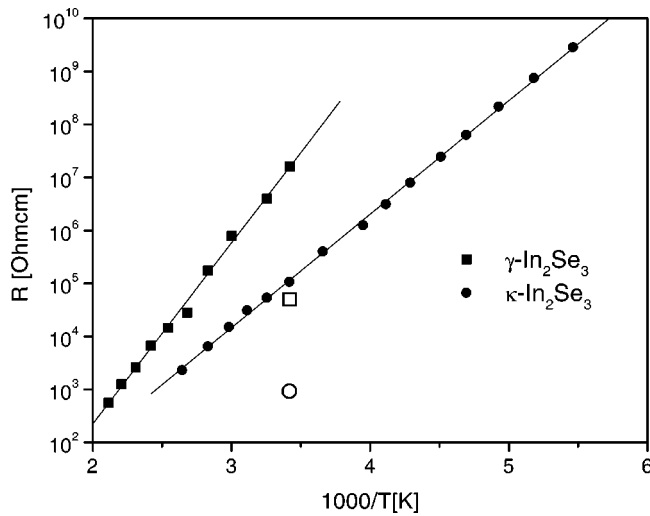


FIG. 5. Temperature dependence of the dark resistivity of κ - In_2Se_3 and γ - In_2Se_3 . The lines are fits based on an Arrhenius behavior of the resistivity with the activation energy being 0.43 and 0.68 eV for κ - In_2Se_3 and γ - In_2Se_3 , respectively. Photoconductivity values at room temperature are indicated by open symbols.

thin metallic (In rich top) layer. The small leakage current compared to the photocurrent indicates possible application in photovoltaic cells for both structures.

Attempts have been made to determine the sign and concentration of the charge carriers by Hall-effect measurements. Neither κ - In_2Se_3 nor γ - In_2Se_3 films showed any Hall effect. Although the high resistance hampered the experiments, a value for the mobility above $1 \text{ cm}^2 \text{ V}^{-1} \text{ s}^{-1}$ could have been detected. A resistivity governed by scattering at the grain boundary, as proposed in Refs. 6, 9, and 14, would explain the absence of Hall effect without invoking unrealistic low mobilities. This process can also lead to an Arrhenius behavior of the temperature dependence of the resistivity. Hot probe tests (Seebeck effect) show that $n_e \mu_e^2 > n_h \mu_h^2$ for both structures.

Optical absorption A was calculated from reflectivity R and transmission T using $A = T/(1-R)$ and the absorption coefficient is subsequently given by $\alpha = -\ln(A)/t$, where t is the film thickness. The absorption curves are shown in Fig. 6 for γ - In_2Se_3 , κ - In_2Se_3 and amorphous In_2Se_3 . In theory, the optical gap can be derived from extrapolating the linear part of $(\alpha h\nu)^n$ versus $h\nu$ where n depends on whether the film has a direct or indirect transition. In reality, however, this procedure is subject to strong ambiguities, and we prefer to report on the isoabsorption gap, where $\alpha = 10^3 \text{ cm}^{-1}$.²⁰ A small, but discernible difference exists between γ - In_2Se_3 and κ - In_2Se_3 . The absorption edge of γ - In_2Se_3 is 1.9 eV in

TABLE II. Resistance and photocurrent of In_2Se_3 . ρ is the dark resistivity, I_l the photocurrent, and I_l/I_d the ratio of photocurrent over dark current I_d . PC is the current per light intensity, assuming an estimated 20% focus of the laser and 30% absorption (from optical measurements).

	$\rho(\Omega \text{ cm})$	$I_l \text{ (A)}$	I_l/I_d	PC (A/W)
γ - In_2Se_3	1.57×10^7	1.3×10^{-8}	419	1.6×10^{-4}
κ - In_2Se_3	1.09×10^5	7.0×10^{-7}	140	1.3×10^{-2}

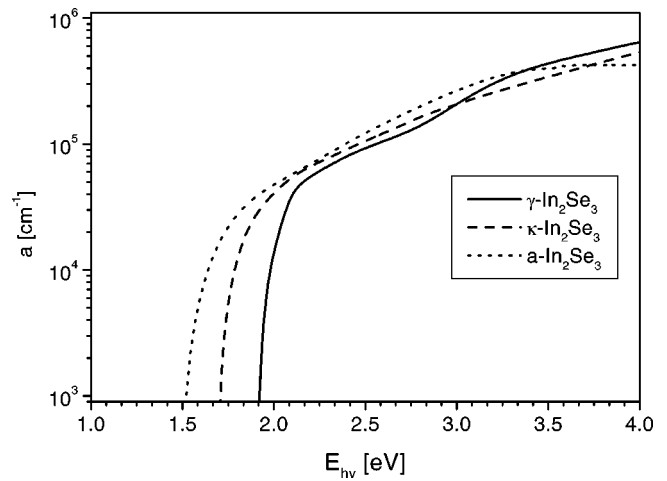


FIG. 6. Optical absorption of 200 nm films of γ - In_2Se_3 , κ - In_2Se_3 , and amorphous In_2Se_3 . The energy at which the absorption is 10^3 cm^{-1} is 1.9, 1.75, and 1.5 eV, respectively.

agreement with literature,²¹ while κ - In_2Se_3 has an absorption edge of 1.75 eV. Both values of the optical gap are considerably higher than twice the activation energy for electrical conduction of the respective structures. This means that the electrical activation energy either probes the grain boundary barrier height or the difference between a donor level and the conduction band edge.

IV. CONCLUSION

Thin films of In_2Se_3 have been prepared by thermal co-evaporation. When annealed *in situ* without a cap layer, the film crystallizes in and up to now, unknown structure. This structure has an x-ray diffraction pattern corresponding to a single interplanar spacing and can be indexed with consecutive 00l peaks. Only when the films are capped with a thin oxide layer (by evaporation or by natural oxidation) before annealing will the reportedly stable γ - In_2Se_3 form, single phase and aligned along the c axis. Rutherford backscattering confirms an In to Se ratio of 2 to 3 for both structures. The new structure has a much lower resistivity than the γ - In_2Se_3 structure, while both structures show large photoconductivity.

ACKNOWLEDGMENTS

The authors would like to thank J. Shervinsky at Harvard University for RBS assistance, and P. Klaumann, T. McClure, and E. Shaw at the MIT/CMSE shared facilities for their support.

¹M. A. Kenawy, H. A. Zayed, and A. M. A. El-Soud, J. Mater. Sci.: Mater. Electron. **1**, 115 (1990).
²S. T. Lakshmikumar and A. C. Rastogi, Sol. Energy Mater. Sol. Cells **32**, 7 (1994).
³P. C. Newman, J. Phys. Chem. Solids **23**, 19 (1962).
⁴J. Ye, S. Soeda, Y. Nakamura, and O. Nittono, Jpn. J. Appl. Phys., Part 1 **37**, 4264 (1998).
⁵M. Yudasaka, T. Matsuoka, and K. Nakanishi, Thin Solid Films **146**, 65 (1987).

- ⁶G. Micocci, A. Tepore, R. Rella, and P. Siciliano, *Phys. Status Solidi A* **148**, 431 (1995).
- ⁷B. Thomas, *Appl. Phys. A: Solids Surf.* **54**, 293 (1992).
- ⁸J. Fotsing, C. Julien, M. Balkanski, and K. Kambas, *Mater. Sci. Forum* **1**, 139 (1988).
- ⁹C. Julien, M. Eddrief, K. Kambas, and M. Balkanski, *Thin Solid Films* **137**, 27 (1986).
- ¹⁰T. Ohtsuka, T. Okamoto, A. Yamada, and M. Konagai, *Jpn. J. Appl. Phys., Part 1* **38**, 668 (1999).
- ¹¹M. Parlak and C. Ercelebi, *Thin Solid Films* **322**, 334 (1998).
- ¹²M. A. Afifi, N. A. Hegab, and A. E. Beksheet, *Vacuum* **46**, 335 (1995).
- ¹³Y. Watanabe, S. Kaneko, H. Kawazoe, and M. Yamana, *Phys. Rev. B* **40**, 3133 (1989).
- ¹⁴J. C. Bernède, S. Marsillac, and A. Conan, *Mater. Chem. Phys.* **48**, 5 (1997).
- ¹⁵M. Emziane and R. Le Ny, *J. Phys. D* **32**, 1319 (1999).
- ¹⁶G. G. Gospodinov, *Thermochim. Acta* **82**, 367 (1984).
- ¹⁷H. Haeuseler and M. Himmrich, *Z. Anorg. Allg. Chem.* **535**, 13 (1986).
- ¹⁸D. Eddike, A. Ramdani, G. Brun, J. C. Tedenac, and B. Liautard, *Mater. Res. Bull.* **33**, 519 (1998).
- ¹⁹M. Emziane and R. le Ny, *Thin Solid Films* **366**, 191 (2000).
- ²⁰D. E. Sweenor, S. K. O'Leary, and B. E. Foutz, *Solid State Commun.* **110**, 281 (1999).
- ²¹C. Julien, A. Chevy, and D. Sapkas, *Phys. Status Solidi A* **118**, 553 (1990).